Estuarine, Coastal and Shelf Science 340 (2026) 110075

Contents lists available at ScienceDirect

Estuarine, Coastal and Shelf Science

journal homepage: www.elsevier.com/locate/ecss

A stable isotope approach to assess the ecological role and fate of macroalgal decomposition in the Antarctic benthos

Nadia Frontier [a,b,*,1], Gabriele Stowasser [a], Chris Harrod [b], Lloyd S. Peck [a], David K.A. Barnes [a], Sebastián Rosenfeld [c,d], Anna M. Jażdżewska [e], Sofie Spatharis [b], Helen Campbell [f], Gloria Dos Santos Pereira [f], Simon A. Morley [a]

[a] British Antarctic Survey, Natural Environment Research Council, Cambridge, England, CB3 0ET, United Kingdom
[b] University of Glasgow, School of Biodiversity, One Health and Veterinary Medicine, Glasgow, Scotland, G12, 8QQ, United Kingdom
[c] Cape Horn International Center (CHIC), Puerto Williams, Chile
[d] Instituto Milenio Biodiversidad de Ecosistemas Antárticos y Subantárcticos, Santiago, 7800003, Chile
[e] Department of Invertebrate Zoology and Hydrobiology, Faculty of Biology and Environmental Protection, University of Łódź, Łódź Voivodeship, Lodz, 90-236, Poland
[f] UK Centre for Ecology & Hydrology, Lancaster Environment Centre, Lancaster, England, LA1 4AP, United Kingdom

ARTICLE INFO

Keywords:
Blue carbon
isotope dual-labelling
Macroinvertebrate assemblages
Glacial retreat
Macroalgal detritus

ABSTRACT

Around Antarctica, disturbance from iceberg scouring and natural macroalgal senescence result in the accumulation of macroalgal detrital material. This detritus in turn supports a significant abundance of detritivorous invertebrates and provides material for carbon burial and sequestration. We tested the hypotheses that decomposing macroalgal detritus makes an increasing contribution to both macroinvertebrate diet, and subsurface sediment organic matter. We analysed data from two independent *in situ* decomposition experiments conducted at Rothera Research Station in two successive years. Mesh cages, containing macroalgal detritus isotopically enriched in 13C and 15N were deployed at an Antarctic soft sediment site. Numerical abundances of macroinvertebrate species as well as the isotopic contribution of macroalgae to macroinvertebrates and sediments were estimated across four-time intervals for each experiment. Thirty-six (2021) and eighty-nine (2022) macroinvertebrate species were associated with experimental cages of macroalgal detritus. Multivariate and univariate analyses revealed temporal shifts in the macroinvertebrate assemblages within each study year, switching from amphipod to mollusc species-dominated assemblages throughout the experiment. The 15N enriched macroalgal detritus were incorporated within benthic sediment and macroinvertebrate tissue. Only the diet of arthropods was influenced by temporal macroalgal decomposition. Isotope measurements of local macroalgal accumulation in sediments showed contrasting trends in both experiments, either declining or accumulating over time with the more less chemically defended macroalgae contributing most to local sediment enrichment. Assessing the fate of macroalgal carbon is important in the polar regions where macroalgal biomass and its detritus are increasing in coastal habitats due to climate change opening new ice-free suitable habitat.

1. Introduction

Globally, marine macroalgae form some of the most extensive and productive coastal habitats, providing crucial ecosystem services (Duarte et al., 2022; Pessarrodona et al., 2022; Eger et al., 2023). Macroalgae not only provide habitat heterogeneity but are an important food source both directly (through consumption) and indirectly, through the assimilation of macroalgal-derived tissue into prey for higher food web species (Dunton, 2001; Corbisier et al., 2004; Leclerc et al., 2013). In addition, macroalgae fix and store inorganic carbon (e.g. from carbon dioxide and bicarbonate) in their tissues and the burial of macroalgal detritus is recognised as a key global pathway for blue carbon sequestration (Filbee-Dexter et al., 2024). Its importance is starting to be recognised in the polar regions (Deregibus et al., 2023; Krumhansl et al.,

* Corresponding author. British Antarctic Survey, Natural Environment Research Council, Cambridge, England, CB3 0ET, United Kingdom.
E-mail addresses: frontier.nadia@gmail.com (N. Frontier), gsto@bas.ac.uk (G. Stowasser), chris.harrod@glasgow.ac.uk (C. Harrod), lspe@bas.ac.uk (L.S. Peck), dkab@bas.ac.uk (D.K.A. Barnes), sebastian.rosenfeld@ug.uchile.cl (S. Rosenfeld), anna.jazdzewska@biol.uni.lodz.pl (A.M. Jażdżewska), sofie.spatharis@glasgow.ac.uk (S. Spatharis), HelCam@ceh.ac.uk (H. Campbell), mdgds@ceh.ac.uk (G.D.S. Pereira), smor@bas.ac.uk (S.A. Morley).
[1] Present address: Swansea University, Singleton Park, Swansea, SA2 8 PP

https://doi.org/10.1016/j.ecss.2026.110075
Received 2 April 2026; Received in revised form 12 June 2026; Accepted 19 June 2026
Available online 23 June 2026

2025).

The fate and transport of macroalgal detritus and its potential for blue carbon sequestration is driven by biological and physical processes (Brouwer, 1996; Queirós et al., 2019; Wright et al., 2022; Simpkins et al., 2025). Macroalgal biomass both resides in coastal habitats and/or is exported beyond the photic zone. This material is subject to disintegration, death and decomposition, and these collective processes exhibit substantial influence upon macroalgal 'detritus' across time (Findlay, 2021). Physically, detritus is formed via macroalgal blade erosion, natural senescence (Krumhansl and Scheibling, 2012), and dislodgement of whole individuals during storms (de Bettignies et al., 2013), as well as iceberg scouring, a process unique to the polar regions (Barnes and Souster, 2011; Barnes, 2017). Although generating a somewhat lower proportion of detrital biomass (Brouwer, 1996), biophysical mechanisms of macroalgal detrital production are also driven by 'messy eating' from invertebrate grazing on macroalgae. This process is difficult to observe and measure, consequently it has not yet been demonstrated in macroalgal source material, but see Møller et al. (2003), and Saba et al. (2011) for examples of wasteful ('sloppy') consumption on phytoplankton sources. Furthermore, macroalgal material is locally re-mineralised by invertebrate consumers, through respiration, excretion and decomposition (Filbee-Dexter et al., 2020), and this process extends to detached macroalgae in the form of detritus (de Bettignies et al., 2020a).

Investigating the dynamics of macroalgal decomposition is especially important in the polar regions where glacial retreat and reduced sea ice results in the colonisation of newly ice-free areas by macroalgae and the wider distribution of macroalgal-derived detritus (Quartino et al., 2013; Deregibus et al., 2023; Amsler et al., 2025). Carbon inputs from macroalgae in the region can be a persistent resource due to the year-round presence of macroalgal detritus (Dieckmann et al., 1985), in contrast to the marked seasonal variation in pelagic primary production by phytoplankton in the Antarctic (Clarke, 1988; Clarke et al., 2014). From an ecological perspective, this process is particularly important for the polar regions, where food input from pelagic primary production is strikingly limited in winter and macroalgae may be the dominant energy source for many marine consumers (Wiencke et al., 2007). From a blue carbon perspective, year-round trophic interactions between macroinvertebrate consumers and macroalgal detritus will have implications for the transfer of polar macroalgal biomass into carbon sinks, where the proportion of non-mineralised macroalgae from consumers has the potential to supply material for deep carbon burial. Measurements of $\delta^{13}C$ and $\delta^{15}N$ isotope ratios of Antarctic nearshore fauna have shown that the assimilated diet of some benthic consumers (herbivorous molluscs and crustaceans) relies exclusively upon sources of macroalgal carbon, hypothesised to be consumed via detrital pathways (Dunton, 2001; Norkko et al., 2004). *In situ* single snap shot in time approaches using dual isotopes such as carbon and nitrogen (Wiencke and Amsler, 2012), and *ex situ* continuous approaches (Braeckman et al., 2019), have highlighted the importance of including temporal dynamics, especially when understanding macroalgal decomposition and its relative role in directly and indirectly fuelling multiple trophic levels and carbon sinks.

A range of macroinvertebrates not only use macroalgae as habitat but also directly consume macroalgae (Dunton, 2001; Aumack et al. 2011, 2017). There is a lack of Antarctic studies assessing the potential temporal variation in the macrofaunal assemblage associated with macroalgal detritus. Our first hypothesis was to examine whether the composition of the macroinvertebrate assemblage changed across time, shifting from pioneering species such as amphipods to gastropods. Our second hypothesis was to test if a reduction in macroalgal C:N ratios in response to decomposing macroalgal was correlated with increased consumption from macroinvertebrate consumers. Macroalgal decomposition, and subsequent changes in food quality (assessed by elemental ratios of carbon and nitrogen (C:N)) may influence macroinvertebrate consumption, although relationships are not always clear (Reichardt and Dieckmann, 1985; Norderhaug et al., 2006). Our third hypothesis tested increasing species-specific macroalgal consumption from a range of representative macroinvertebrate taxa over time, with an expected greater response detected in non-chemically defended macroalgae compared to chemically defended species. A large proportion of Antarctic macroalgal species contain chemical defence compounds, with greater occurrences reported in polar macroalgae compared to those in temperate and tropical regions (Amsler et al., 2005). As macroalgae decompose, it has been hypothesised that their palatability to consumers increases in response to a breakdown of secondary metabolites, such as phlorotannins and terpenes (Dieckmann et al., 1985; Amsler et al., 2005). However, relationships between specific chemical defences which deter grazers and their relation to macroalgal decomposition have not yet been defined. Understanding macroinvertebrate consumption between a range of chemically and non-defended macroalgal in the form of detritus is still in its infancy (Amsler et al., 2009), and warrants further investigation across a broader range of macroalgal sources and macroinvertebrate taxa.

The fourth and final hypothesis will test the prediction of increasing values of isotopically enriched 13C and 15N macroalgal detritus across time into sub-surface sediments. The fate and burial of macroalgae detritus remains a key topic for assessing and ground-truthing the potential for carbon sequestration (Krumhansl et al., 2025). The visual detection of macroalgal detritus within Antarctic deep coastal sediments (at ca. 1500 - 2000 m) has provided crucial evidence for macroalgal carbon sequestration potential (Reichardt, 1987; Fischer and Wiencke, 1992). However, the temporally driven physical and biological decomposition of macroalgal detritus into particulate and dissolved organic matter may not always be detectable from visual observations alone (Brouwer, 1996). Extending observational evidence, modern ecological tools, such as environmental DNA, and particle tracking allow predictions of macroalgal carbon inputs from various forms of detritus, from dissolved organic carbon (DOC) to particulate organic carbon (POC) (Queirós et al., 2019; Krumhansl et al., 2025). The current study examines temporal variation in the contribution of macroalgal detritus into subtidal sediments from isotopically labelled macroalgal detritus due to natural fragmentation and invertebrate consumption.

Empirical knowledge regarding the mechanisms supporting polar macroalgal blue carbon pathways is currently missing. Using a carbon and nitrogen dual stable isotope labelling approach, this study aims to assess the fate and ecological role of isotopically enriched macroalgal detritus to test four hypotheses. These findings have the potential to improve polar-specific assessments about the fate of macroalgal detrital carbon from two key decomposition pathways in coastal Antarctic benthic ecosystems, namely macroinvertebrate consumption and local sediment burial potential. In accordance with future predictions of glacial retreat and reduced sea ice cover in the polar regions (Barnes et al., 2020), as well as increased iceberg scouring of the shallows (Barnes et al., 2025), there are likely to be increased macroalgal subsidies for macroinvertebrates and increased material available for potential carbon sequestration.

2. Materials and methods

2.1. Experimental introduction

Four locally abundant and accessible (by SCUBA diving) species of macroalgae were selected to test of hypotheses: *Iridaea* sp., *Trematocarpus antarcticus, Palmaria decipiens and Desmarestia menziesii* (Table 1), and subjected to *in situ* Antarctic decomposition experiments. Previous studies in the polar regions have demonstrated that macroalgal detritus decomposition with time (Supporting **inf**ormation, Fig. S1a) occurs at rates much slower than temperate macroalgae (White and Norkko, 2025b). Remaining biomass can be converted into decay rates (D): (Equation (1)) (Supporting **informa**tion, Fig. S1b).

$$D_t = D_0 e^{-kt} \quad \text{[Equation 1]}$$

Table 1
Ecological information about four species of macroalgae used in the *in situ* decomposition experiments. Herbarium images of macroalgae from Mystikou et al. (2014) for *Iridaea* sp. and *P. decipiens* and Küpper et al. (2019) (Küpper et al., 2019)for *D. menziesii* and the Algal Herbarium Portal from Lamb (1965) for *T.antarcticus.*

Species/Class	Depth (m)	Strategy	Morphology	Description	Chemical defence
Desmarestia menziesii J. Agardh 1848 Heterokontophyta (brown) 	5–20 m, juveniles up to 30 m (Küpper et al., 2019).	Season anticipator[a] Endemic to Antarctica (including Sub Antarctica).	Adult, max length 3 m, main axis, opposite, occasionally alternate, branching fronds (Wiencke et al., 1995). Juveniles, distinctly smaller, their lateral branches more pinnate (feathery) in appearance compared to adults (Küpper et al., 2019).	Major canopy forming species, attached to rocky substratum (Küpper et al., 2019).	Highly chemically defended Amsler et al., (2020).
Iridaea sp. (Turner) Bory, 1826 Rhodophyta (red) 	0–30 m (Wiencke and Amsler, 2012).	Season responder[b] Temperate and polar distribution.	Flat, single broad frond. Holdfast is a flat disk with a flat stipe of 1-4 cm in length (Wiencke and Clayton, 2002).	Attached to rocky substrata, common in the lower inter-tidal and subtidal (Martín et al., 2016). Patchily distributed.	Chemically defended (Amsler et al., 2020).
Palmaria decipiens (Reinsch) R.W. Ricker, 1987 Rhodophyta (red) 	0–100 m (Robinson et al., 2022; Wiencke and Amsler, 2012).	Season anticipator[a] Grows predominantly in late winter and spring. Annual species. Endemic to Antarctica (including Sub Antarctica).	Blades oblong, lanceolate, often waxy at margins with slippery, glossy surface, reddish or purplish pink. Narrow stipe (Wiencke and Clayton, 2002).	Attached to rocky substrata (Wiencke and Clayton, 2002)	Not chemically defended (Amsler et al., 2020).
Trematocarpus antarcticus (Hariot) Fredericq & R.L. Moe, 2009 Rhodophyta (red) 	5–33 m (Hommersand et al., 2009).	Season anticipator[a] Endemic to Antarctica (including Sub Antarctica).	Branching, flattened species (Wiencke and Clayton, 2002),	The species occurs on rocky substrata, mixed with Terebellidae *sp.* mats and frequently seen as detached material on live urchin spines (Author observations).	Not chemically defended (Amseler et al. 2005; Amsler et al., 2020).

[a] Season anticipators begin growth under short-day conditions in late winter/spring, often in low light under sea-ice. Maximal growth occurs in spring.
[b] Season responders start growth and reproduction later than season anticipators with favourable spring/summer light conditions (Wiencke and Amsler, 2012).

Where macroalgae biomass remaining at time t, D_t, is a function of exponential decay with rate constant k, of remaining biomass D_0.

2.2. Experimental design overview

In situ experimentation was conducted adjacent to the British Antarctic Survey's Rothera Research Station at a regularly visited dive site in Ryder Bay (67° 35.743′ S, 68° 15.246′ W), South of Adelaide Island, located to the west of the West Antarctic Peninsula (Fig. 1).

To capture interannual variability, two long-term *in situ* macroalgal decomposition experiments were deployed at a depth of 17 m at a soft-sediment site between January 2021–December 2022 (Fig. 1). Each experiment was sampled at four fixed time points when weather and sea-ice conditions permitted. Consequently, Experiment 1 and Experiment 2 were sampled across different sampling intervals, which limits comparisons to general trends across time, rather than between equal sampling intervals. A total of 20 mesh cages were deployed across each experiment (Fig. 2) containing isotopically enriched macroalgae (**see** supporting information S1 **for isotope enrichment methods**). Macroalgae were packed into cages representing a single layer of plant (reducing self-shading effects and maintaining water flow) so that the surface area of all cages were lined with macroalgae but that macroalgae were not packed on-top of each other to reduce anoxia. Specifically, Experiment 1 assessed decomposition dynamics for three macroalgal species, *P. decipiens, T. antarcticus, D. menziesii,* in mixed cages containing macroalgae (n = 16 macroalgae cages, n = 4 control cages). Control mesh cages which did not contain macroalgae were deployed alongside the mesh treatment cages to quantify the presence of invertebrates in substrata lacking macroalgal detritus. Experiment 2 contained an additional macroalgae species, *Iridaea* sp., following *in situ*

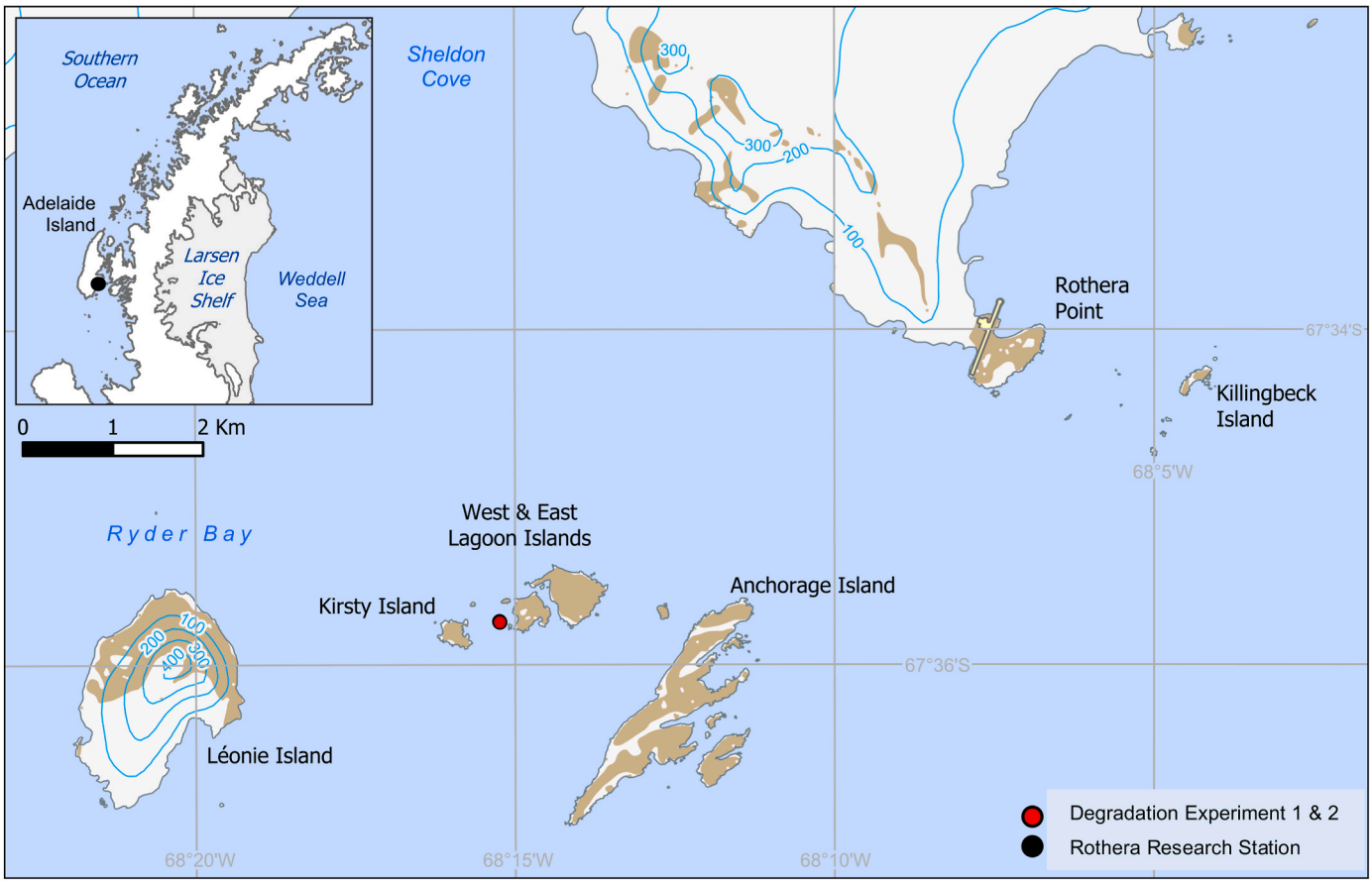

Fig. 1. Map of the study area showing the location of Experiments 1 and 2 (red dot) and the location of Ryder Bay (black dot on insert) relative to the West Antarctic Peninsula. Produced by the Mapping and Geographic Information Centre, © British Antarctic Survey, UK Research and Innovation, 2023. Data from the SCAR Antarctic Digital Database, 2023. (For interpretation of the references to colour in this figure legend, the reader is referred to the Web version of this article.)

SCUBA surveys in 2022 which confirmed the presence of *Iridaea* sp. as a locally dominant macroalga. In this experiment, macroalgal detritus was assigned to macroalgal-species specific mesh cages to obtain macroalgal species-specific macroinvertebrate assemblages, and mixed macroalgal detrital mesh cages. Experiment 1 only contained mixed-macroalgal mesh cages.

2.3. Experimental deployment

Experiment 1 and Experiment 2 were deployed to the Southeast of Lagoon Island (67° 35.743′S, 68° 15.246′W) (Fig. 1) where macroalgal detritus covered on average 11.1% (SE ± 1.2), or and 31.45 (SE ± 6.7) m^2, of the seafloor between 15 and 18 m depth (Supporting information, Fig. S2). Experiment 2 was deployed 100 m south of the first experiment, with little tidal upstream or downstream influence, of Experiment 1 (67° 35.74′S, 68° 15.241′W) to reduce the chance of contamination from enriched macroalgae in Experiment 1.

For each decomposition experiment, twenty mesh cages (30 cm × 15 cm x 1 cm) were constructed from 0.5 mm plastic mesh. Five mesh cages were attached to a 1.5 m length of chain at 15 cm intervals, totalling four chain lengths per experiment (Fig. 2). Cages either contained macroalgae collected from South Cove and Cheshire Island (Fig. 1) or were deployed at randomly selected positions along the chains as empty control cages (Experiment 1). Each cage was assigned a unique identification code.

For Experiment 1 (2021) and Experiment 2 (2022) initial macroalgal wet masses (T_0) were variable due to the selection of whole individual macroalgae, including holdfasts (Experiment 1: 67 - 105 g per cage; Experiment 2, 94 - 252 g per cage). Macroalgae were not subject to artificial cutting to a standardised size to avoid unnaturally accelerating the decomposition process. Therefore, the starting masses of macroalgae were recorded for each cage and biomass metrics were normalised by calculating the relative later biomass loss or gain, after removing any macroinvertebrates and/or epiphytes.

2.4. Temporal sampling

Experiment 1 was deployed in January 2021, and sampled, using SCUBA, at four time points in February, March, April and October 2021. The following year in February 2022, Experiment 2 was subsequently deployed and similarly sampled at four intervals in March, April, November and December 2022 (Fig. 2).

During each sampling event, five mesh cages were sampled from one chain replicate. SCUBA divers carefully removed each cage from the chain and placed them in a fine mesh collection bag (75 μm pore size) to capture the macroalgal content and its associated macroinvertebrates. Where possible, triplicate sediment samples were collected, using falcon tubes with 2 cm width. Samples of the surface 2 cm were collected under and adjacent to each treatment cage, including control cages in Experiment 1. If time permitted, control sediment samples were collected within ~10 m of the experimental site. Treatment cages wrapped in independent fine mesh collection bags, were transferred to a box of ambient seawater on the boat to avoid cross-contamination and later stored in the Bonner Laboratory flow-through aquarium.

Macroalgal contents from each cage were placed in a sieve for 5 min and weighed to obtain wet mass (Sartorius LA3200D, ±0.001 g). Biomass measurements may contain bacterial communities and/or biofilm growth. As a result, typical methods to remove water

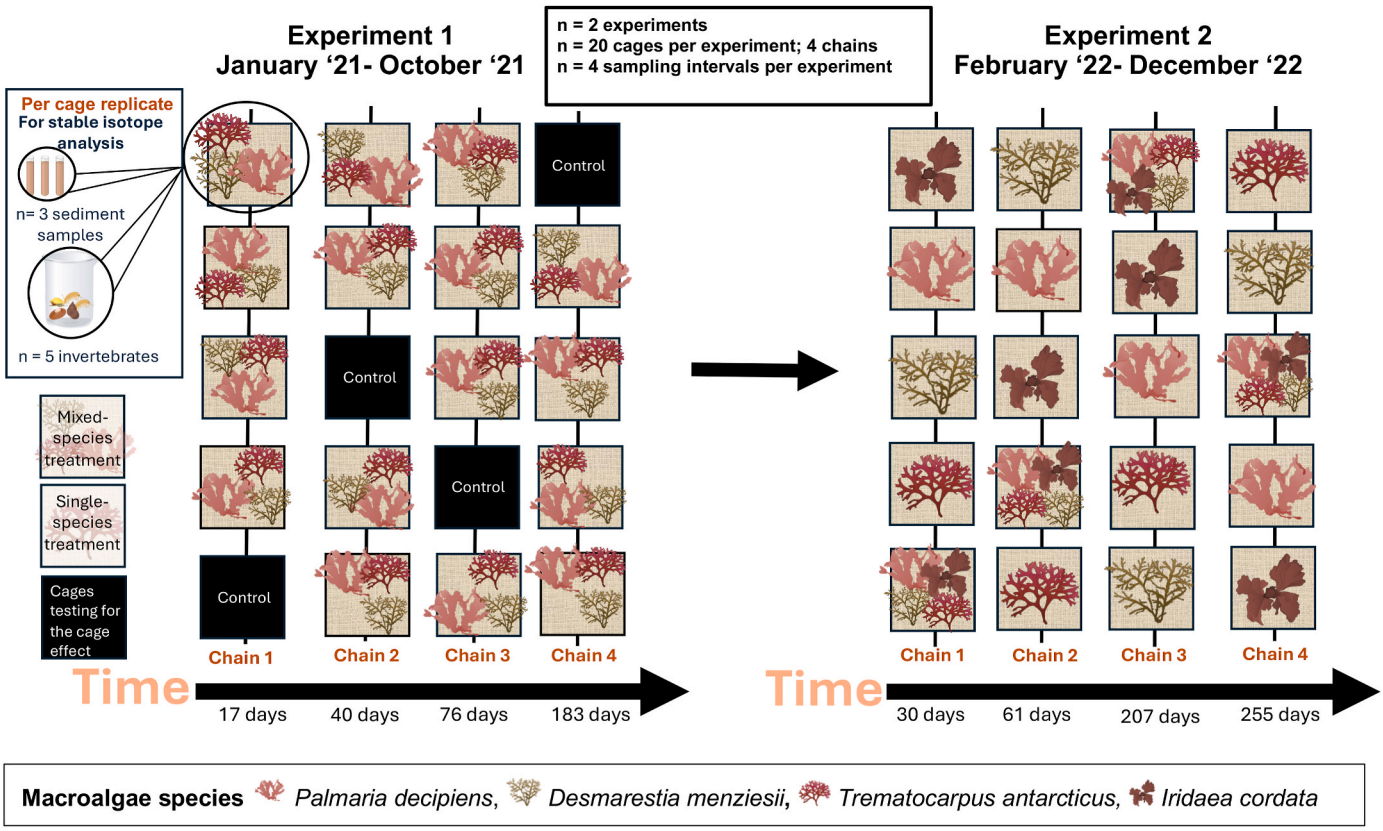

Fig. 2. A schematic of two *in situ* decomposition experiments. Both experiments were sampled across four time points. Black boxes indicate a control cage without any macroalgae to assess potential cage-effects on macroinvertebrate assemblages. Experiment 1 contained mesh bags with mixed macroalgal species (*Desmarestia menziesii, Palmaria decipiens* and *Trematocarpus antarcticus*), whilst Experiment 2 contained a mixture of single species and mixed macroalgal species in mesh bags with the addition of *Iridaea cordata*.

(centrifugation or blotting) were not employed to avoid removing crucial elements of the decomposition process. Macroalgae were dried to a constant mass at 60°C and reweighed to obtain dry mass.

2.5. Samples for stable isotope analysis

Each treatment cage and fine mesh collection bag was carefully opened and rinsed over a 1 mm sieve to obtain any macroinvertebrates. The sample contents were emptied into a sorting tray, and all macroinvertebrate consumers were sorted into larger taxonomic groups and identified to either species or genus level. However, amphipods collected during Experiment 1 were only identified to order level due to amphipods preservation difficulties from Experiment 1 (Taxonomic keys used are presented in supporting **information,** Table S1). From each treatment cage, 5 and 15 individuals of the common taxa were kept for stable isotope analysis in addition to a subsample of sediment from each triplicate falcon tube and a small subsection of enriched macroalgae was removed from each cage (see supporting information S1 for detailed isotope sample preparation methods).

2.6. Data analysis

Data were analysed in R (V. 4.4.1; R Core Team, 2025) using the R Studio interface.

2.6.1. Macroinvertebrate assemblage analysis, multivariate frequentist approach

To test the hypothesis that macroinvertebrate assemblage composition changes in response to macroalgal detritus decomposition over time, multivariate analyses were conducted with i) all species at the species level (Experiment 2) and aggregated under the phyla ii) Arthropoda, iii) Mollusca, iv) Annelida and v) Echinodermata. Chordata and Cnidaria were only recorded at one of four time points and due to the lack of replication, were excluded from the analysis. Due to differences in the biomass of macroalgae placed in each cage at the onset of the experiment, macroinvertebrate abundance data was normalised according to the initial starting biomass of macroalgae per cage (Equation (2)).

$$Taxa\ normalised\ abundance^{n} = \frac{Taxa\ count^{n}}{T_0\ macroalgae\ biomass} \qquad \text{[Equation 2]}$$

Where n = a unique species/group and T_0 represents the macroalgae biomass pre-deployment into the field.

Due to the presence of three abundant gastropods, *Skenella paludinoides*, *Eatoniella strebeli* and *Eatoniella caliginosa* (with abundances sometimes exceeding 2000 individuals per cage), data were fourth-root transformed to down-weigh the contribution of dominant species for the purpose of multivariate analyses based on the Bray-Curtis dissimilarity index (Bray and Curtis, 1957). Potential variation in assemblage composition was examined visually through ordination, using Principal Coordinate Analysis (PCoA) (*vegan* package, V. 2.7.1). Dissimilarity between potential groupings of samples was visualised using the two PCoA axes which explained the greatest variation in shaping assemblage dissimilarity. Statistical differences in assemblage composition between groups were examined through permutation-based multiple analysis of variance of Bray-Curtis dissimilarities, PERMANOVA (Anderson, 2001), through the *adonis2* routine in *vegan*. Nine separate *adonis* models were conducted on separate groupings of data for the PCoA analysis. Homogeneity of multivariate dispersion (differences in group dispersion) were tested using the 'betadisperser' function in *vegan*. If grouping variables

(time points) satisfied assumptions of homogeneity of multivariate dispersion, post hoc comparisons were manually extracted from the *adonis* model. The Echinodermata and Annelida present were not considered for further analysis because only phyla with groupings that displayed temporal variation in assemblage structure were used.

For i) all phyla ii) Arthropoda and iii) Mollusca, eigenvalues were interrogated to determine the 10 most influential species in driving macroinvertebrate assemblage dissimilarity across four time points. Influential species were extracted from the PCoA analyses and displayed on two-dimension plots using vectors. The length of the vector (shown as an arrow) is proportional to the influence of the species and the direction of the arrow points towards which time groupings the species most influenced.

2.6.2. Macroinvertebrate assemblage analysis, control cages

When assessing the multivariate assemblage composition of control cages from Experiment 1 relative to experimental macroalgae cages, a separate dataset contained macroinvertebrate abundances from control and experimental cages, and two approaches were taken which included all macroinvertebrate phyla i) abundances were analysed per cage unit where each cage was a standardised floor area of 0.045 m^2 and ii) abundances were converted to presence/absence of macroinvertebrate species.

To further assess the effect of control cages, in Experiment 1, a separate dataset calculated species abundance and species richness from control and experimental macroalgae cages according to the area of each cage, 0.045 m^2. Species richness represents the number of distinct species per cage replicate. Model residuals were inspected for uniformity, dispersion and autocorrelation (*DHARMa* package V. 0.4.7) (Hartig et al. 2025).

2.6.3. Stable isotope mixing models for macroinvertebrates, Bayesian approach

Bayesian stable isotope mixing models (Parnell et al., 2013; Phillips et al., 2014) were used to estimate the relative contribution of enriched food sources to macroinvertebrate consumers under different experimental conditions. Experimental treatments relied on the use of enriched carbon and nitrogen stable isotopes to label algae, which range far beyond natural abundance values and complicate mixing models (Fry, 2006). To overcome this, fractional abundance values of carbon and nitrogen isotopes were used in the mixing models (*simmr*, V 0.5.1.217) (Parnell et al., 2013). Macroinvertebrate consumers were considered as mixtures and mean ± SD $\delta^{13}C$ and $\delta^{15}N$ values of enriched macroalgae and enriched sediment from Experiment 1 and Experiment 2 represented source contributions in the mixing model. Control cages (no macroalgae) were excluded from models assessing macroinvertebrate consumption. Due to the use of enriched labelled isotopes which would not detect subtle changes in temporal variation (Fry et al., 2004; de Bettignies et al., 2020a), source values were combined for enriched macroalgae over time. Furthermore, because of the use of enriched labelled isotopes, data were not adjusted for trophic enrichment between consumers and their putative diet (Fry, 2006). Pelagic natural abundance sources from Ryder Bay (zooplankton, POM) (G. Stowasser and N.Z werschke, pers. comms 12.08.25, *unpublished data*) and natural abundance sources (control sediment, control macroalgae) were trialled in a separate SIMMR model but due to the nature of the enrichment experiment, only enriched sources were included in the final model (supporting **infor**mation, Fig. S3).

To maximise replication across all time points, *simmr* models were constructed with consideration of four phyla: Arthropoda (n = 99), Mollusca (n = 35), Echinodermata (n = 37) and Annelida (n = 37). The model calculated the relative contribution of each enriched experimental macroalgae and enriched sediment to the diet of consumers across four time points within each experiment.

Mixing models were built in *simmr* using 20,000 iterations where the first 1000 values were burnt, and 4 chains were produced. Posterior predictive checks were conducted on each *simmr* model and correlation matrices were examined between source inputs to ensure correlations between sources did not exceed 60%. Due to the paucity of understanding about macroalgae species-specific detrital contributions to macroinvertebrate diet, uninformative priors were given to the *simmr* model (20% per source contribution) with a standard deviation of 10%.

2.6.4. Stable isotope mixing models for sediment, Bayesian approach

To test whether macroalgae accumulated locally in coastal sediment or were exported, sediment stable isotope data were treated in the same way as macroinvertebrate data. $\delta^{13}C$ and $\delta^{15}N$ values were converted to Fractional Abundance values (F). A further *simmr* mixing model was run with sediment treated as the mixture and using the different macroalgae as potential sources allowed an estimation of the fate of macroalgae in surface sediments (2 cm). Due to the proximity of control cages (no macroalgae) to experimental cages, control cages contained enriched signals of macroalgae and therefore control cage sediment samples were included in the model. The *simmr* model used default uniform priors for macroalgal contribution to sub-surface sediment as the model was successfully able to resolve differences between the macroalgae sources. Correlation matrices between sources did not exceed 35%.

Within each experiment (Experiment 1, n = 31; Experiment 2, n = 32), $\delta^{13}C$ and $\delta^{15}N$ values were compared across time points and treatments (treatment cage sediment, control cage sediment, experimental site sediment (10m away)) using general linear models, *GLMs*, and analysis of variance, *ANOVA*. Model assumptions were satisfied using *DHARMa* and differences between time points were assessed using the *emmeans* function (emmeans package, V 1.10.5) (Lenth and Piaskowski, 2025) and represented graphically.

3. Results

At the end of the experiment, of the macroalgae tissue which non-degraded, the tissue was photosynthetically active with F_vF_m values, a proxy for photosynthetic performance, reported to be above 0.6 for all macroalgal species until 255 days (data not shown). Due to low currents and sedimentation around the study side, macroalgal fragment in mesh bags did not accumulate sedimentation throughout the study period and received maximum light.

Thirty-six macroinvertebrate species were identified from Experiment 1 and eighty-nine species were identified from Experiment 2 (supporting information, Fig. S4). Common and abundant species comprised the gastropods *Skenella paludinoides*, *Altenaeum charcoti, Margarella antarctica* and *Iothia emarginuloides,* a bivalve *Philobrya wandelensis*, isopods *Cymodocella tubicauda, Munna antarctica,* amphipods *Oradarea* sp., *Prostebbingia* sp., an echinoid *Sterechinus neumayeri* and a holothuroid *Cucumaria georgiana*.

3.1. Temporal changes in macroinvertebrate assemblage composition

PCoA1 and PCoA2 axes explained at least 40% of the dissimilarity in assemblage composition across both experiments at the resolution of all species, Arthropoda and Mollusca (Fig. 3). No differences across time were detected in assemblage composition for Echinodermata or Annelida (data not shown) across both Experiment 1 and Experiment 2.

For Experiment 1, 52% of assemblage dissimilarity was explained by the first two axes when taxa were aggregated at phylum level (n = 37). Time had a significant effect on macroinvertebrate assemblage composition (PERMANOVA, $F_{3,15} = 4.0$, $P < 0.001$). Post hoc comparisons showed there were significant differences (<0.05) between all time point comparisons, except for between day 40 and day 76 (PERMANOVA, day40: day76, $F_{1,3} = 1.72$, $p = 0.06$) (Fig. 3a). Similarity in assemblage composition between sampling day 40 and 76 were most strongly characterised by two isopods, *Munna antarctica* and *Cymodocella tubicauda* and the amphipods identified to the taxonomic resolution of order. 69% of assemblage dissimilarity was explained when sub-

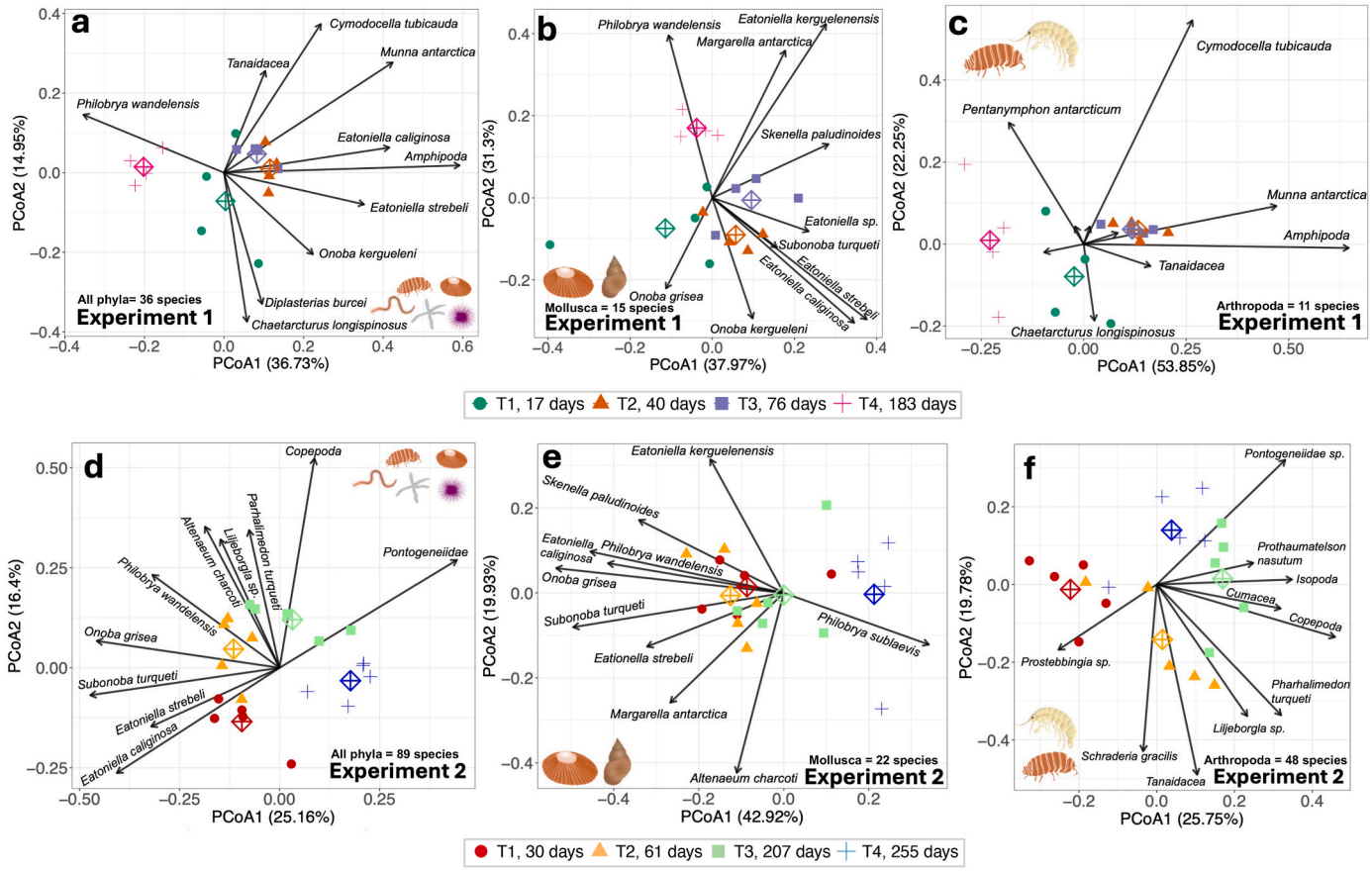

Fig. 3. Variation in macroinvertebrate assemblage composition (species abundances) over time across Experiment 1 shown through Principal Coordinate Analysis (PCoA) ordination for all phyla (a, c), the Mollusca phylum only (b, e) the Arthropoda phylum only (c, f). Abundances were normalised to initial macroalgae biomass present within each cage. Data were fourth root transformed. Coloured crosses represent the mean for each time point. Vectors (arrows) and depict the 10 most influential species in driving assemblage dissimilarity between time points, the length of the arrows reflect the relative importance of this strength.

grouping mollusc species (n = 16 species). Similarly, the analysis of variance in the mollusc assemblage showed an overall significant effect of time (PERMANOVA, $F_{3,15} = 4.26$, $p < 0.001$). Post hoc comparisons showed significant differences ($p < 0.05$) between all time point comparisons other than day 17 and day 40 (PERMANOVA, day17:day40, $F_{1,3} = 2.33$, $p = 0.07$) and day 17 and day 76 (PERMANOVA, day17:day76, $F_{1,3} = 3.33$, $p = 0.06$) (Fig. 3b). The mollusc species *Eatoniella strebeli* and *Eatoniella caliginosa* were the strongest drivers of assemblage dissimilarity between day 40 and day 76 whilst the molluscs *Eatoniella kerguelensis* and *Philobrya wandelensis* influenced assemblage dissimilarity at sampling day 183. When grouping the arthropod phylum, 76% of assemblage dissimilarity was explained (n = 11 species) and amphipods were only identified to the taxonomic resolution of order, limiting direct comparisons with Experiment 2 due to preservation-limitations in Experiment 1. Nevertheless, the permutational multivariate analysis of variance showed an overall significant effect of time (Time, $F_{3,15} = 5.5$, $p < 0.001$). Post hoc comparisons showed significant differences between time point comparisons except for day 17 and day 183 (day17:day183, $F_{1,3} = 3.0$, $p = 0.06$) and between day 40 and day 76 (day40:day76, $F_{1,3} = 1.45$, $p = 0.27$). The latter is evident from Fig. 3c where mean centroids overlap.

For Experiment 2, 42% of assemblage dissimilarity was explained when grouping phyla and using the PCoA1 and PCoA2 axes. Time has a significant on assemblage composition (PERMANOVA, $F_{3,19} = 3.40$, $p < 0.001$). The post hoc test showed significant differences in overall assemblage composition between all sampling intervals (Fig. 3d). The permutational multivariate analysis of variance in the mollusc assemblage composition explained 62% of assemblage dissimilarity and demonstrated an overall significant effect of time on assemblage composition (PERMANOVA, $F_{3,19} = 3.86$, $p < 0.001$). Post hoc comparisons showed significant differences between sampling intervals except for between day 61 and day 207 (T2:T3, $F_{1,3} = 1.44$, $p = 0.19$) (Fig. 3e). When grouping arthropod species, 46% of assemblage dissimilarity was explained. Arthropod assemblage composition was consistently influenced by time (Time, $F_{3,19} = 3.37$, $p < 0.001$) and post hoc comparisons showed significant differences ($p < 0.05$) between assemblage composition at each of the four experimental time periods (Fig. 3f).

For Experiment 2, the permutation multivariate analysis of macroinvertebrate assemblage variation, using specific macroalgae (n = 4) and mixed cages of macroalgae (n = 1), explained 42% of assemblage dissimilarity. This study detected no apparent effect of macroalgae macroalgal composition on macroinvertebrate assemblage composition (Macroalgal composition, $F_{4,19} = 0.76$, $p = 0.87$) (supporting information, Fig. S5). From Experiment 1, permutation multivariate analysis of variation comparing control cages and macroalgal treatment cages, when data were analysed according to density and presence/absence group, showed that control cages did not cluster as a separate statistically significant group (Supporting information, Fig. S6a and S6b). Post-hoc comparisons of treatment within each time point were not possible due to lack of replication.

3.2. Temporal consumption of macroalgal detritus from macroinvertebrates

Macroinvertebrate species assimilated enriched isotopes into their

tissues with detections of enriched macroalgal detritus in >50% of samples at each sampling interval using 13C and 15N labelling. Stable isotope mixing models were successful in resolving temporal differences in arthropods (Fig. 4a) whilst there was limited success in resolving temporal differences in molluscs, echinoderms and annelids (Fig. 4b, c & d). Stable isotope values were pooled together for the Arthropoda, including orders such as amphipods and isopods, which represented the most abundant orders from experimental cage assemblages. For Experiment 1, the results of the mixing model showed the most important detrital source to arthropod macroinvertebrate diet was *P. decipiens*. When considering the maximal mean contribution of source to arthropod diet, the mixing model estimated *P. decipiens's* source contribution as 39% (95% credibility intervals 17- 63%). A temporal element was detected with increasing contributions of *P. decipiens* to arthropod diet between sampling intervals: 31% at day 17 (13- 55%), 35% (15-60%) at day 40, 39% (17- 63%) at day 76 before reducing to 32% (14-57%) at day 183. Experiment 2 introduced a different macroalgal source into the experiment and the mixing model revealed high proportions of *Iridaea* sp. in consumer diet with maximal median contribution of 0.56% (24-81%). Temporal changes were less pronounced across time with proportional contributions of 59% (29-83%) at day 30, 54% (21-80%) at day 61, 56% at day 207 (24-81%) and 33% (8-66%) at day 205.

3.3. Local sediment accumulation of macroalgae detritus

Temporal differences in $\delta^{15}N$ sediment values (collected under experimental cages) were detected across both experiments, with time-specific difference in Experiment 1 (ANOVA, $F_{3,43} = 22.40$, $p = <0.001$), driven by initially high values at 40 days followed by a subsequent decline in enrichment for the following time points ($t_{3,42} = -8.0$, $p < 0.001$). In contrast, time specific differences in Experiment 2 (ANOVA, $F_{3,44} = 18.18$, $p = <0.001$) (Fig. 5a) were dominated by higher enriched $\delta^{15}N$ values towards the end of the experiment at 207 days ($t_{3,44} = 5.20$, $p < 0.001$) (Fig. 5a). Overall, there were higher levels of 15N isotopic enrichment of macroalgae in Experiment 2 (maximum

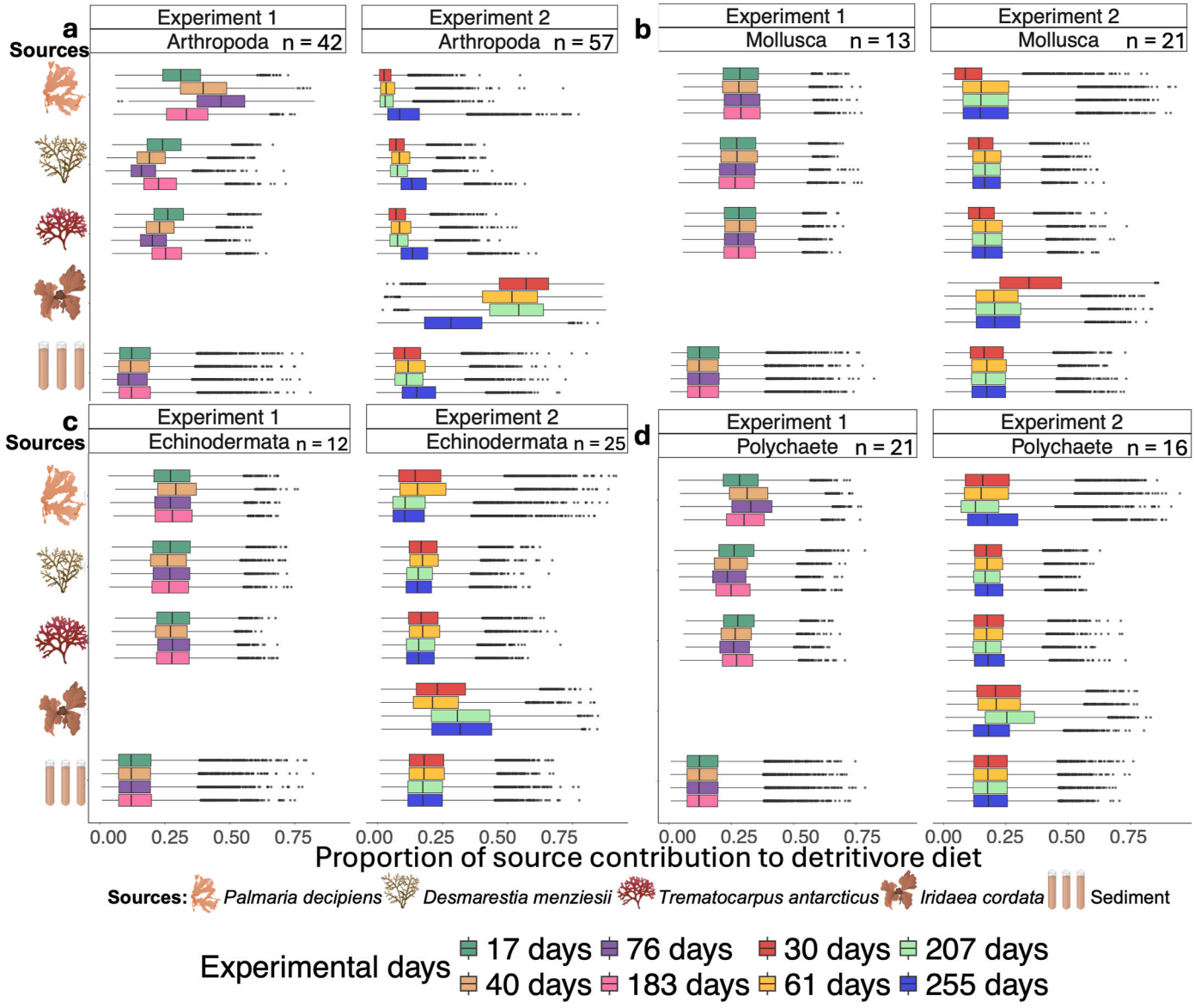

Fig. 4. SIMMR mixing model contributions for a) Arthropoda b) Mollusca c) Echinodermata d) Annelida using five source contributions (n = 4 macroalgae, n = 1 sediment). Output from SIMMR. Boxes show interquartile ranges, horizontal lines indicate the median and black points represent data outside of the interquartile range. Model made with non-informative priors set to 0.2 for each source with a standard deviation of 0.1 for each prior. The number of isotope samples are listed by each phyla per experiment.

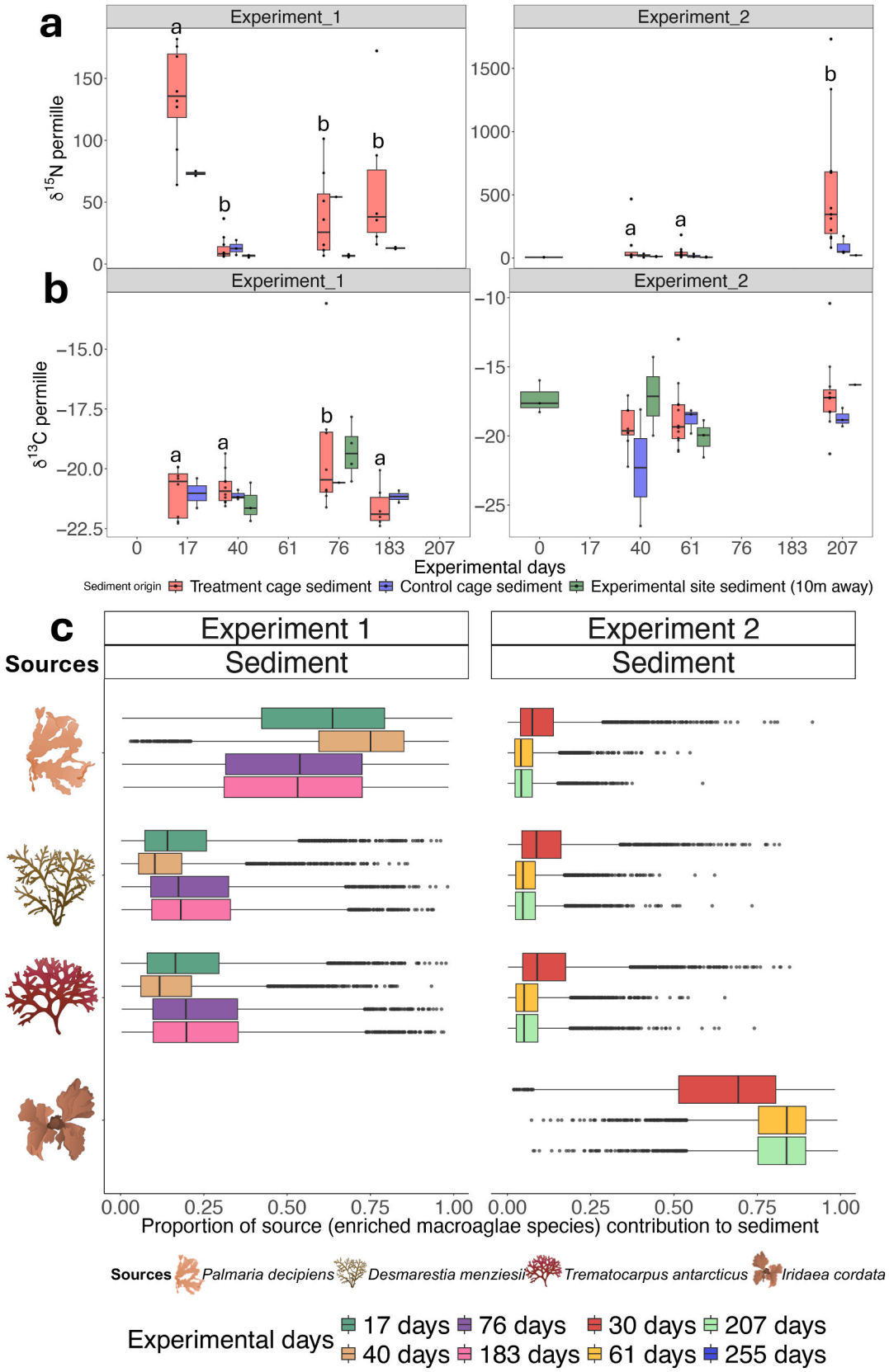

Fig. 5. a) δ15N values and b) δ13C values in sediment collected from enriched cages (n = 63) and control cages and experimental site cages shown as a reference. c) SIMMR mixing model contributions for enriched macroalgae to sediment under experiment cages. Boxes show interquartile ranges, horizontal lines indicate the median and black points represent data outside of the interquartile range. Uniform default priors were used in the model. Output from SIMMR. Sediment samples were not collected on day 255 from Experiment 2.

$\delta^{15}N$ value = 1731‰) compared to Experiment 1 (maximum $\delta^{15}N$ value = 75‰) due to species-specific differences in uptake of the enriched isotopes.

Due to differences in the physiological uptake of isotope signatures (macroalgae have reduced affinity for 13C compared to 15N), $\delta^{13}C$ sediment values (collected under experimental cages) remained similar within the sub-surface sediment throughout in Experiment 2 (ANOVA, $F_{3,44} = 2.37$, $p = 0.08$) but not in Experiment 1 (ANOVA, $F_{3,43} = 5.11$, $p < 0.01$), driven by higher values at day 76 ($t_{3,43} = 2.75$, $p < 0.01$) (Fig. 5b). Following 15N enrichment, $\delta^{13}C$ values were also consistently higher for Experiment 2 compared to experiment 1 (ANOVA, $F_{1,93} = 22.06$, $p < 0.001$).

Sediment samples collected either under control cages (no enriched macroalgae) for Experiment 2, showed similar signs of enrichment (maximum value $\delta^{15}N = 173‰$) compared to the macroalgae containing cages (Fig. 5a and b). This finding demonstrates the local transport of enriched macroalgal detritus into adjacent sediment. Sediment samples collected around the experimental site (located 10 m from the experiment) showed limited signs of enrichment from experimental macroalgae (maximum value $\delta^{15}N$ = 22‰), providing confidence that the 100 m distance separating Experiment 1 and Experiment 2 avoided isotopic contamination.

The Bayesian stable isotope mixing model successfully revealed that labelled macroalgae contributed to the organic content of sediments collected below experimental cages, although limited changes were detected across time. *Palmaria decipiens's* maximum contribution to sediment macroalgal detection was 69% at day 40 (17- 95%) for Experiment 1 and the addition of *Iridaea* sp. in Experiment 2 shifted the balance of the dominant macroalgae to 81% at day 61 (49- 96%). When both *P. decipiens's* and *Iridaea* sp. were included in the model, *Iridaea* sp. contributed most to local sediments compared to other macroalgae species (Fig. 5c).

4. Discussion

Polar coastal regions are a hotspot of physical change where macroalgae, and its fate, may become increasingly important (Mystikou et al., 2014; Filbee-Dexter et al., 2024). In this study, we provided *in situ* insight into the fate of Antarctic macroalgal detrital decomposition from an ecological and blue carbon perspective in an Antarctic coastal soft sediment habitat at 17 m depth. *In situ* experimentation demonstrated an effect of time upon: macroalgae decomposition, detritivore assemblage composition, increased reliance upon macroalgal detritus in arthropod diet, and in one experiment, sub-surface sediment accumulation. Results from this study are timely because climate change is driving glacial retreat, reduced sea ice in time and space and increasing ice scouring in Antarctica (Barnes et al., 2025). Changes in Antarctic benthic ecosystems include predicted increases in macroalgal biomass, and its resultant detritus, in response to the increased light availability (both in area and duration) and new ice-free habitat (Barnes et al., 2020; Deregibus et al., 2023).

In accordance with previous macroalgal detrital studies from polar (Brouwer, 1996) and temperate regions (de Bettignies et al., 2020a; Wright et al., 2022), macroalgal biomass in this study generally decreased over time, with the exception of *Trematocarpus antarcticus* which consistently increased over time in Experiment 1 (Supporting **infor**mation, Fig. S1a). Macroalgal decomposition of *Desmarestia menziesii* was faster in this experiment, than reported from an Antarctic congeneric *Desmarestia anceps* (Brouwer, 1996). Subtidal decomposition rates of macroalgae (decomposition constant k = 0.01 - 0.04) in this study were slower than in temperate and tropical regions (k = 0.01 - 0.5) (White and Norkko, 2025a) (Supporting **informat**ion, Fig. S1b)**.** Growth of macroalgae post detachment from the substratum is not uncommon and has been documented in the Antarctic macroalga, *Desmarestia menziesii,* at 5 m depth and for *D, anceps* at 17 m (Amsler et al., 2012; Fairhead et al., 2006). However, macroalgal detritus also occurs at depths far beyond 5 m (Supporting **inform**ation, Fig. 2). At the depth of this study, 17 m, irradiances decreased to ~5% of irradiance at the surface (Supporting **infor**mation, Table S3). A standard view of irradiance decay with depth does not capture seasonal variability. It also does not allow for shading from other macroalgal fragments in detrital accumulations (Garrido et al., 2023) that further attenuates light and thus accelerates macroalgal decomposition. Although the assemblage composition of macroalgal-associated microbes were not explicitly measured in this study, it is possible that they were partly responsible for macroalgal decomposition observed in the current work. The observed decomposition rates of Antarctic macroalgae suggest a substantial proportion of material is available for i) consumption by associated macroinvertebrate assemblages ii) possible burial into sediments and iii) decomposition into POM and DOM in the water column or sediment, similar to processes to those reported in some temperate ecosystems (de Bettignies et al., 2020a; Wright et al., 2022; Krumhansl et al., 2025).

4.1. Macroinvertebrate abundance

In accordance with our hypothesis, the experimental macroalgal detrital resource was generally of decreasing importance for amphipod species over time as it decomposed. We obtained maximum comparable amphipod densities (23 amphipods g^{-1}) with other polar studies which documented up to 20 amphipods g^{-1} of algal fresh wet mass (Takeuchi and Watanabe, 2002; Huang et al., 2007). A temporal reduction in amphipod abundance across both experiments supports the role some amphipods have as pioneering species in using largely pre-decomposed macroalgae, however, these results are based only on correlative assumptions. In both experiments, there was a disproportionate influence from the dominant mollusc, the gastropod, *Skenella paludinoides,* in most cage replicates (Supporting **i**nformation, Fig. S4**).** This finding accords with an East Antarctic study which identified *S. paludinoides* as the dominant gastropod associated with the macroalga, *Desmarestia chordalis* (Takeuchi and Watanabe, 2002), suggesting an affinity of this species with both attached, and decomposing detrital material.

4.2. Multivariate analysis of macroinvertebrate assemblage composition

Macroalgal detritus offers subsidies and structural complexity to adjacent habitats which may be nutrient poor (Lastra et al., 2014). In accordance with our hypothesis, our results showed that differences in macroinvertebrate assemblage composition over time, correlated with changes in macroalgal biomass. Many species in the current study were found to be similar to previously documented macroalgal assemblages (Aumack et al., 2011; Schram et al., 2016). This study also found that macroalgal species-specific detritus exerted no effect on macroinvertebrate assemblage composition. This suggests that the general ecological role of macroalgal detritus in driving assemblage composition dissimilarity is likely temporal (Supporting **information**, Fig. S5). The two experiments were not conducted over directly comparable sampling intervals (Experiment 1: 17, 40, 76, 183 days; Experiment 2: 30, 60, 207, 255 days), but they were deployed in mid austral summer (January and February) in consecutive years and so the influence of inter-annual variability between experiments may have been an important driver. A phytoplankton bloom of greater magnitude and duration occurred before sampling was conducted in Experiment 2, with 80 days above 2.5 mg m^3 Chla between December 2021 and March 2022 compared with 37 days above 2.5 mg m^3 Chla between December 2020 and March 2021 (Supporting information, Fig. S7).

The effect of control cages, which did not contain any macroalgae, potentially confounds the assumed driver of macroalgal decomposition. Multivariate analyses using macroinvertebrate abundance from control and treatment cages, normalised to either cage area or presence and absence of macroinvertebrate species, showed clustering of control cages with experimental cages across some sampling intervals (Supporting **in**formation, Fig. S6). This indicates that in addition to

macroalgal detrital material, artificial substrate can provide habitat heterogeneity associated with macrofauna biodiversity. To disentangle the inevitable cage effect associated with litter bag studies, we adopted a dual experimental approach by combining the numerical abundances of macroinvertebrates with their stable isotope signature, to permit the evaluation of macroalgal dietary benefit to consumers.

4.3. Macroalgal decomposition

Macroalgal C:N ratios have been documented to decrease during decomposition (Reichardt and Dieckmann, 1985; Norderhaug et al., 2006), indicating a progressively higher proportion of nitrogen compared to carbon. This phenomenon can serve as a proxy for microbial decomposition, where microbes degrade detrital biopolymers and increase the nutritive value of detrital carbon for macro-heterotrophic consumers (Reichardt and Dieckmann, 1985; Brouwer, 1996; Norderhaug et al., 2006), in conjunction with an increase in tissue nitrogen from nitrogen based decay-resistant compounds (Brouwer, 1996; de Bettignies et al., 2020b). We found species-specific C:N ratios and temporal trends for Antarctic macroalgae. *T. antarcticus* exhibited the lowest C:N ratios of the macroalgal species studied which is consistent with C:N ratios from other polar studies (Amsler et al., 2005). The relative C:N ratios did not change over time in *Iridaea* sp. and *T. antarcticus* and therefore this response cannot be linked to changes in macroinvertebrate chemical-defences and thus assumed consumer palatability influencing decomposition, over time. These results are contrary to some studies which did not detect changes in C:N ratios during the course of macroalgal decomposition (Reichardt and Dieckmann, 1985; Norderhaug et al., 2006) whilst other studies did detected changes in C:N ratios in macroalgae (Brouwer, 1996; de Bettignies et al., 2020a). A temporal increase in C:N ratios were observed in the highly chemically defended species *D. menziesii,* whilst variation in the C:N relationship for *P. decipiens* presented a consistent trend across time *(*Supporting information, Fig. S1c). Although trends were similar across both experiments, differences were most pronounced in Experiment 2 which suggests the influence of interannual unmeasured environmental variables between both experiments. The temporal changes for *P. decipiens* are likely to have exerted ecological implications for macroinvertebrate consumption. Lower C:N ratios may, alternately, reflect carbon assimilation by macroinvertebrates over time, which is further reflected in the sharp temporal decrease in biomass for *P. decipiens (*Supporting information, Fig. S1a).

4.4. Tracing of dual-labelled stable macroalgal 13C and 15N isotopes in macroinvertebrates

The use of labelled 13C and 15N isotopes permitted a mechanistic ecological insight into the temporal consumption of macroalgal detritus over time and was used in models to assess the contribution of different sources to consumer diet. Antarctic macroalgae had a greater affinity for 15N compared to 13C and enrichment was more pronounced in $\delta^{15}N$ values. Bayesian stable isotope mixing models (SIMMR), using $\delta^{13}C$ and $\delta^{15}N$ isotope ratios from enriched macroalgae and associated macroinvertebrates, did not support the hypothesis of increased detrital assimilation over time, when considering the macroinvertebrate phyla which were sampled. The current experiment showed that time-dependent effects were resolved from SIMMR models in arthropod species, but the increased consumption of macroalgae was not detected in nearshore Antarctic representatives of the Mollusca, Echinodermata and Annelida. Notably, the introduction of a chemically defended macroalgal source, *Iridaea* sp.*,* provided a stronger contribution to arthropod diet in Experiment 2 (Fig. 4). Furthermore, macroinvertebrate consumption from experimental macroalgal detritus was not the only source fuelling the food web, because although a higher proportion of arthropod diet was fuelled by experimental macroalgal detritus, Echinodermata, Mollusca and Annelida did not use macroalgal detritus as a food source in the current study. Our arthropod consumption result aligns with a polar *ex situ* study, documenting increased consumption during macroalgal detrital decomposition in amphipods (Reichardt and Dieckmann, 1985; Amsler et al., 2012). However, even within arthropods functional roles vary widely where feeding strategies such as shredding, grazing, suspension feeding and deposit-feeding will likely impact the fate of macroalgal detritus, but the resolution of species-specific temporal sampling in this study currently limits these conclusions to phyla (Schaal et al., 2016). Aligning these results with the temporal shifts documented in macroinvertebrate assemblage composition from PCoA analyses, demonstrates that factors other than diet, can cause shifts in the assemblage composition within the Mollusca phyla (Fig. 3b–e). In contrast, the observed temporal changes in arthropod diet may have been largely responsible for our assemblage composition result which aggregated all phyla (Fig. 3a–c).

4.5. Tracing of dual-labelled stable macroalgal 13C and 15N isotopes in coastal sediments

The Bayesian stable isotope mixing model revealed that labelled macroalgae contributed to the organic content of sediments collected below experimental cages. *Palmaria decipiens* and *Iridaea* sp. contributed most to local sediments compared to other macroalgae (Fig. 5). We observed the predicted increase of macroalgal detrital accumulation in local sediments in Experiment 2, but our hypothesis was not supported in Experiment 1. This study has demonstrated that macroalgal detritus may not only accumulate in coastal sediments, further supporting research showing that detritus has the potential to both be locally consumed, passed into the food webs and exported offshore (Reichardt, 1987; Fischer and Wiencke, 1992; Dunton, 2001). Limited changes were detected across time from the SIMMR model. However, raw $\delta^{15}N$ values demonstrated a temporal difference in enrichment. Experiment 1 experienced a decrease in local sediment enrichment over time whilst Experiment 2 revealed a progressive increase. Opposing trends are perplexing when biomass decline was observed and occurred with time in both experiments (Supporting information, Fig. S1). Given the relatively high abundances of amphipods detected in Experiment 1 compared to Experiment 2, amphipods may have consumed disproportionately more macroalgae in Experiment 1, reducing the availability of macroalgae into sub-surface sediments and resulting in a lack of accumulation of macroalgae into sediments (Fig. 5). Alternatively, biological mechanisms have been identified as key drivers contributing towards the percolation of macroalgae across the water-sediment interface via bioirrigation and bioturbation processes (Queirós et al., 2019). Infauna can rework the sediment, drawing macroalgal particles and solutes across the sediment-water interface, which may have influenced the disparity in results between Experiment 1 and 2. However, these factors were beyond the scope of this study and highlights the difficulties in identifying underlying factors when unmeasured variables are operating across many scales. Finally, δ^{15} N and $\delta^{13}C$ values were consistently higher for Experiment 2 which may have been an artefact of enriched isotope labelling (**see** Supporting **information S1**).

4.6. The role of arthropods in the fate of macroalgal blue carbon and future recommendations

Arthropod macroinvertebrate isotope values revealed an initial increase of assimilated *P. decipiens* in Experiment 1, with similar trends but a greater lag in Experiment 2. *In situ* stable isotope sampling highlighted arthropod consumption in-part driving macroalgal detrital decomposition, and their role as consumers in re-suspending carbon from macroalgal detritus is more important than other consumers, see also (Amsler et al., 2005). This may subsequently impact the proportion of macroalgal carbon entering blue carbon sinks. Of the Arthropoda sampled, Amphipoda were the most abundant (Supporting information, Fig. S4) and their numerical decline across time likely reflects a decline in

macroalgal-derived nutrition (Fig. 5).

Future approaches could improve the experimental design used in the current study. First, the proximity of control cages to experimental cages, containing macroalgal detritus, may have confounded an assessment of the 'cage effect' where mobile macroinvertebrates were increasingly attracted towards experimental cages containing macroalgae, and thus we sampled an 'overspill' effect. The alternative explanation of substrate providing enhanced habitat heterogeneity, whether biological or artificial, cannot be separated from this experimental design. Deploying control cages in litter bag experiments is important but is not always standard practice for *in situ* macroalgal decomposition experiments (de Bettignies et al., 2020a, White and Norkko, 2025b), although the current study is limited by control cage replication across time points ($n = 1$) and an increase in number of control cages would be beneficial. A tentative conclusion of macroalgal detritus supporting elevated biodiversity could be concluded from elevated species richness in macroalgal treatment cages compared to control cages (Supporting information, Fig. S6d). Based on the results of this study, future studies could increase control cage replication at each time interval to gain more power to properly interrogate such a conclusion. Furthermore, *in situ* experimentation prevents the disentanglement of any seasonal or inter-annual effects upon associated macroinvertebrate biodiversity where, in this study two phytoplankton blooms of vastly different magnitudes occurred across the experimental periods (Supporting information, Fig. S7). There would, therefore be a benefit from continuing to conduct future experiments over consecutive, or preferably several years. Amphipods were not identified to species level in Experiment 1, limiting comparisons between both experiments (Fig. 5c) and if possible, species should be identified immediately to prevent potential identification difficulties due to preservation. The use of enriched isotopes permitted the current study to trace the flow of macroalgal detritus, of known detrital age, through trophic levels and into sediment. However, this approach limited the study to using only enriched sources of macroalgae and sediment. An alternative approach could expand the diet of phyla to assess the relative contribution of enriched macroalgae compared to phytoplankton, zooplankton, Ice algae and other potential primary sources with a high affinity towards macroinvertebrates (Supporting information, Fig. S3). Despite converting $\delta^{13}C$ and $\delta^{15}C$ values into units of fractional abundance, enrichment effects may have impacted the performance of the SIMMR models and future studies could run enriched and natural abundance *in situ* experiments in parallel.

To conclude, although global estimates of carbon export from macroalgal habitats have recently included Antarctica (Filbee-Dexter et al., 2024), targeted mechanistic studies investigating the fate of polar macroalgal detritus are sparse, limiting an informed marine conservation and management framework (Macreadie et al., 2021). This study specifically measured the ecological role of macroalgal detritus in supporting macroinvertebrate nutrition, and using stable isotopes provided a quantitative assessment of macroinvertebrate consumption and local sediment burial potential. Enriched stable isotope techniques were successfully used for the first time in a polar environment. This study has demonstrated that enriched macroalgae can accumulate in local sediments. However, there is not a direct link between macroalgae and sediment accumulation which highlights the potential for macroalgal export beyond the photic zone. Although this study has demonstrated some mechanisms associated with the fate and carbon sequestration potential of macroalgal detritus, further research should continue to more accurately estimate the proportion of macroalgal detritus removed and re-suspended via macroinvertebrate consumption, natural macroalgal senescence (including bacterial decomposition) and local sediment accumulation. Specific research targeting these questions will continue to improve calculations concerning macroalgal detrital contributions towards polar blue carbon stocks.

5. Permits

Samples were collected in Antarctica under BAS-S7-2021/01, BAS-S7-2022/01 permits and sent back to the British Antarctic Survey, UK, in accordance with the Plant Health Organisation (PHO) permit.

Funding source

This work was supported by core funding from the NERC, UKRI, UK to the British Antarctic Survey. The analysis of Isotope samples was provided via an independent NERC grant from the NERC Isotope Facility (NEIF) grant number: 2550.1022 awarded in January 2023.

CRediT authorship contribution statement

Nadia Frontier: Conceptualization, Data curation, Formal analysis, Methodology, Writing – original draft, Writing – review & editing. **Gabriele Stowasser:** Methodology, Writing – original draft, Writing – review & editing. **Chris Harrod:** Supervision, Writing – original draft, Writing – review & editing. **Lloyd S. Peck:** Funding acquisition, Methodology, Project administration, Supervision, Writing – review & editing. **David K.A. Barnes:** Supervision, Writing – review & editing. **Sebastián Rosenfeld:** Data curation. **Anna M. Jażdżewska:** Data curation. **Sofie Spatharis:** Supervision, Writing – review & editing. **Helen Campbell:** Methodology. **Gloria Dos Santos Pereira:** Project administration. **Simon A. Morley:** Funding acquisition, Methodology, Project administration, Supervision, Writing – review & editing.

Declaration of competing interest

The authors declare the following financial interests/personal relationships which may be considered as potential competing interests: Nadia Frontier reports financial support was provided by Natural environment research countil. Nadia Frontier reports a relationship with UK Research and Innovation Natural Environment Research Council that includes: funding grants. If there are other authors, they declare that they have no known competing financial interests or personal relationships that could have appeared to influence the work reported in this paper.

Acknowledgements

With thanks to the marine teams of Rothera Research Station from 2020 to 2023, especially Ryan Mathews and Pete Hill. Poppy Brewer, Matt Hughes, Aurelia Reichardt and Louis Day for their assistance with sample processing. Darren Sleep for his technical assistance during stable isotope mass spectrometry analysis at the Centre for Ecology and Hydrology. Rona McGill, Pascal Riera and Ben Wigham for input during the initial conception of the project and to Simon Babayan for statistical insight. We acknowledge the use of the unpublished data from the Rothera oceanographic time series (RaTs) held in the Polar data Centre in the British Antarctic Survey.

Appendix A. Supplementary data

Supplementary data to this article can be found online at https://doi.org/10.1016/j.ecss.2026.110075.

Data availability

Data is available from the British Antarctic Survey Polar Data Center using the following DOI: doi.org/10.5285/c01e2345-4406-404c-bbf2-f1a733077751.

References

Amsler, C.D., Amsler, M.O., Klein, A.G., McClintock, J.B., Iken, K., Galloway, A.W., 2025. Substantial short-term increases in brown macroalgal cover and total macroalgal biomass with decreased sea ice on the Western Antarctic Peninsula. Mar. Ecol. Prog. Ser. 759, 17–34. https://doi.org/10.3354/meps14840.

Amsler, C.D., Amsler, M.O., McClintock, J.B., Baker, B.J., 2009. Filamentous algal endophytes in macrophytic Antarctic algae: prevalence in hosts and palatability to mesoherbivores. Phycologia 48, 324–334. https://doi.org/10.2216/08-79.1.

Amsler, C.D., Iken, K., McClintock, J.B., Amsler, M.O., Peters, K.J., Hubbard, J.M., Furrow, F.B., Baker, B.J., 2005. Comprehensive evaluation of the palatability and chemical defenses of subtidal macroalgae from the Antarctic Peninsula. Mar. Ecol. Prog. Ser. 294, 141–159. https://doi.org/10.3354/meps294141.

Amsler, C.D., McClintock, J.B., Baker, B.J., 2012. Palatability of living and dead detached Antarctic macroalgae to consumers. Antarct. Sci. 24, 589–590. https://doi.org/10.1017/S0954102012000624.

Amsler, C.D., McClintock, J.B., Baker, B.J., 2020. Chemical mediation of antarctic macroalga-grazer interactions. In: Gómez, I., Huovinen, P. (Eds.), Antarctic Seaweeds. Springer, Cham. https://doi.org/10.1007/978-3-030-39448-6_17.

Anderson, M.J., 2001. A new method for non-parametric multivariate analysis of variance. Austral Ecol. 26, 32–46. https://doi.org/10.1111/j.1442-9993.2001.01070.pp.x.

Aumack, C.F., Amsler, C.D., McClintock, J.B., Baker, B.J., 2011. Changes in amphipod densities among macroalgal habitats in day versus night collections along the Western Antarctic Peninsula. Mar. Biol. 158, 1879–1885. https://doi.org/10.1007/s00227-011-1700-0.

Aumack, C.F., Lowe, A.T., Amsler, C.D., Amsler, M.O., McClintock, J.B., Baker, B.J., 2017. Gut content, fatty acid, and stable isotope analyses reveal dietary sources of macroalgal-associated amphipods along the western Antarctic Peninsula. Polar Biol. 40, 1371–1384. https://doi.org/10.1007/s00300-016-2061-4.

Barnes, D.K.A., 2017. Iceberg killing fields limit huge potential for benthic blue carbon in Antarctic shallows. Glob. Change Biol. 23, 2649–2659. https://doi.org/10.1111/gcb.13523.

Barnes, D.K.A., Giles, A., Glaz, P., McLoughlin, S., Clement, A., Morley, S.A., 2025. Long term marine biodiversity monitoring in coastal Antarctica: are fewer rare species recruiting? Glob. Change Biol. 31, e70341. https://doi.org/10.1111/gcb.70341.

Barnes, D.K.A., Sands, C.J., Cook, A., Howard, F., Roman Gonzalez, A., Muñoz–Ramirez, C., Retallick, K., Scourse, J., Van Landeghem, K., Zwerschke, N., 2020. Blue carbon gains from glacial retreat along Antarctic fjords: what should we expect? Glob. Change Biol. 26, 2750–2755. https://doi.org/10.1111/gcb.15055.

Barnes, D.K.A., Souster, T., 2011. Reduced survival of Antarctic benthos linked to climate-induced iceberg scouring. Nat. Clim. Change 1, 365–368. https://doi.org/10.1038/nclimate1232.

Braeckman, U., Pasotti, F., Vázquez, S., Zacher, K., Hoffmann, R., Elvert, M., Marchant, H., Buckner, C., Quartino, M.L., Mác Cormack, W., Soetaert, K., Wenzhöfer, F., Vanreusel, A., 2019. Degradation of macroalgal detritus in shallow coastal Antarctic sediments. Limnol. Oceanogr. 64, 1423–1441. https://doi.org/10.1002/lno.11125.

Bray, J.R., Curtis, J.T., 1957. An ordination of the upland Forest communities of Southern Wisconsin. Ecol. Monogr. 27, 326–349. https://doi.org/10.2307/1942268.

Brouwer, P.E.M., 1996. Decomposition in situ of the sublittoral Antarctic macroalga Desmarestia anceps Montagne. Polar Biol. 16, 129–137. https://doi.org/10.1007/BF02390433.

Clarke, A., 1988. Seasonality in the antarctic marine environment. Comp. Biochem. Physiol. A Part B: Comparative Biochemistry 90, 461–473. https://doi.org/10.1016/0305-0491(88)90285-4.

Clarke, K.R., Gorley, R.N., Somerfield, P.J., Warwick, R.M., 2014. Change in marine communities. An Approach to Statistical Analysis and Interpretation, third ed. PRIMER-E Ltd, pp. 41–48.

Corbisier, T.N., Petti, M.A.V., Skowronski, R.S.P., Brito, T.A.S., 2004. Trophic relationships in the nearshore zone of Martel Inlet (King George Island, Antarctica): δ13C stable-isotope analysis. Polar Biol. 27, 75–82. https://doi.org/10.1007/s00300-003-0567-z.

de Bettignies, F., Dauby, P., Lepoint, G., Riera, P., Bocher, E., Bohner, O., Broudin, C., Houbin, C., Leroux, C., Loisel, S., Davoult, D., 2020a. Temporal succession of a macrofaunal community associated with kelp fragment accumulations in an *in situ* experiment. Mar. Ecol. Prog. Ser. 656, 109–121. https://doi.org/10.3354/meps13391.

de Bettignies, F., Dauby, P., Thomas, F., Gobet, A., Delage, L., Bohner, O., Loisel, S., Davoult, D., 2020b. Degradation dynamics and processes associated with the accumulation of *Laminaria hyperborea* (Phaeophyceae) kelp fragments: an in situ experimental approach. J. Phycol. 56, 1481–1492. https://doi.org/10.1111/jpy.13041.

de Bettignies, T., Wernberg, T., Lavery, P.S., Vanderklift, M.A., Mohring, M.B., 2013. Contrasting mechanisms of dislodgement and erosion contribute to production of kelp detritus. Limnol. Oceanogr. 58, 1680–1688. https://doi.org/10.4319/lo.2013.58.5.1680.

Deregibus, D., Campana, G.L., Neder, C., Barnes, D.K.A., Zacher, K., Piscicelli, J.M., Jerosch, K., Quartino, M.L., 2023. Potential macroalgal expansion and blue carbon gains with northern Antarctic Peninsula glacial retreat. Mar. Environ. Res. 189, 106056. https://doi.org/10.1016/j.marenvres.2023.106056.

Dieckmann, G., Reichardt, W., Zielinski, D., 1985. Growth and production of the seaweed, *Himantothallus grandifolius*, at King George Island. In: Siegfried, W.R., Condy, P., Laws, R.M. (Eds.), Antarctic Nutrient Cycles and Food Webs. Springer, Berlin, pp. 104–108. https://doi.org/10.1007/978-3-642-82275-9_15.

Duarte, C.M., Gattuso, J.-P., Hancke, K., Gundersen, H., Filbee-Dexter, K., Pedersen, M. F., Middelburg, J.J., Burrows, Michael T., Krumhansl, K.A., Wernberg, T., Moore, P., Pessarrodona, A., Ørberg, S.B., Pinto, I.S., Assis, J., Queirós, Ana M., Smale, D.A., Bekkby, T., Serrão, Ester A., Krause-Jensen, D., 2022. Global estimates of the extent and production of macroalgal forests. Global Ecol. Biogeogr. 31, 1422–1439. https://doi.org/10.1111/geb.13515.

Dunton, K.H., 2001. δ15N and δ13C measurements of antarctic peninsula fauna: Trophic relationships and assimilation of benthic seaweeds. Am. Zool. 41, 99–112. https://doi.org/10.1668/0003-1569(2001)041[0099:NACMOA]2.0.CO;2.

Eger, A.M., Marzinelli, E.M., Beas-Luna, R., Blain, C.O., Blamey, L.K., Byrnes, J.E., Carnell, P.E., Choi, C.G., Hessing-Lewis, M., Kim, K.Y., Kumagai, N.H., 2023. The value of ecosystem services in global marine kelp forests. Nat. Commun. 14, 1894. https://doi.org/10.1038/s41467-023-37385-0.

Fairhead, V.A., Amsler, C.D., McClintock, J.B., Baker, B.J., 2006. Lack of defense or phlorotannin induction by UV radiation or mesograzers in *Desmarestia anceps* and *D. menziesii* (Pharophyceae). J. Phycol. 42, 1174–1183. https://doi.org/10.1111/j.1529-8817.2006.00283.x.

Filbee-Dexter, K., Pedersen, M.F., Fredriksen, S., Norderhaug, K.M., Rinde, E., Kristiansen, T., Albretsen, J., Wernberg, T., 2020. Carbon export is facilitated by sea urchins transforming kelp detritus. Oecologia 192, 213–225. https://doi.org/10.1007/s00442-019-04571-1.

Filbee-Dexter, K., Pessarrodona, A., Pedersen, M.F., Wernberg, T., Duarte, C.M., Assis, J., Bekkby, T., Burrows, M.T., Carlson, D.F., Gattuso, J.-P., Gundersen, H., Hancke, K., Krumhansl, K.A., Kuwae, T., Middelburg, J.J., Moore, P.J., Queirós, A.M., Smale, D. A., Sousa-Pinto, I., Suzuki, N., Krause-Jensen, D., 2024. Carbon export from seaweed forests to deep ocean sinks. Nat. Geosci. 17, 552–559. https://doi.org/10.1038/s41561-024-01449-7.

Findlay, S.E.G., 2021. Organic matter decomposition. In: Weathers, K.C., Strayer, D.L., Likens, G.E. (Eds.), Fundamentals of Ecosystem Science, second ed. Academic Press, pp. 81–102. https://doi.org/10.1016/B978-0-12-812762-9.00004-6.

Fischer, G., Wiencke, C., 1992. Stable carbon isotope composition, depth distribution and fate of macroalgae from the Antarctic Peninsula region. Polar Biol. 12, 341–348. https://doi.org/10.1007/BF00243105.

Fry, B., 2006. Stable Isotope Ecology. Springer, New York. https://doi.org/10.1007/0-387-33745-8.

Fry, B., Mutchler, T., Sullivan, M.J., 2004. Potential of 14N isotope enrichment to resolve ambiguities in coastal trophic relationships. Mar. Ecol. Prog. Ser. 266, 27–33. https://doi.org/10.3354/meps266027.

Garrido, I., Hawk, H.L., Bruning, P., Pardo, L.M., Johnson, L.E., 2023. Drift algal accumulation in ice scour pits provides an underestimated ecological subsidy in a novel antarctic soft-sediment habitat. Biology 12, 128. https://doi.org/10.3390/biology12010128.

Hartig, F., 2025. DHARMa: residual diagnostics for hierarchical (Multi-Level/mixed) regression models. R package version 0.4.7.

Hommersand, M.H., Moe, R.L., Amsler, C.D., Fredericq, S., 2009. Notes on the systematics and biogeographical relationships of Antarctic and sub-Antarctic Rhodophyta with descriptions of four new genera and five new species. Bot. Mar. 52, 509–534. https://doi.org/10.1515/BOT.2009.081.

Huang, Y.M., Amsler, M.O., McClintock, J.B., Amsler, C.D., Baker, B.J., 2007. Patterns of gammarid amphipod abundance and species composition associated with dominant subtidal macroalgae along the western Antarctic Peninsula. Polar Biol. 30, 1417–1430. https://doi.org/10.1007/s00300-007-0303-1.

Küpper, F.C., Amsler, C.D., Morley, S., de Reviers, B., Reichardt, A., Peck, L.S., Peters, A. F., 2019. Juvenile morphology of the large Antarctic canopy-forming brown alga, *Desmarestia menziesii* J. Agardh. Polar Biol. 42, 2097–2103. https://doi.org/10.1007/s00300-019-02584-3.

Krumhansl, K.A., Lee, K.C., Ma, Y., Wu, Y., Baker, T.H.A., Wong, M.C., Azetsu-Scott, K., Gentleman, W.C., 2025. Pathways of blue carbon export from kelp and seagrass beds along the Atlantic coast of Nova Scotia. Sci. Adv. 11, 1952. https://doi.org/10.1126/sciadv.adw1952.

Krumhansl, K.A., Scheibling, R.E., 2012. Production and fate of kelp detritus. Mar. Ecol. Prog. Ser. 467, 281–302. https://doi.org/10.3354/meps09940.

Lastra, M., Rodil, I.F., Sánchez-Mata, A., García-Gallego, M., Mora, J., 2014. Fate and processing of macroalgal wrack subsidies in beaches of Deception Island, Antarctic Peninsula. J. Sea Res. 88, 1–10. https://doi.org/10.1016/j.seares.2013.12.011.

Leclerc, J.C., Riera, P., Leroux, C., Lévêque, L., Laurans, M., Schaal, G., Davoult, D., 2013. Trophic significance of kelps in kelp communities in Brittany (France) inferred from isotopic comparisons. Mar. Biol. 160, 3249–3258. https://doi.org/10.1007/s00227-013-2306-5.

Lenth, R., Piaskowski, J., 2025. Emmeans: estimated marginal means, aka least-squares means. R package version 2.0.0.

Macreadie, P.I., Costa, M.D.P., Atwood, T.B., Friess, D.A., Kelleway, J.J., Kennedy, H., Lovelock, C.E., Serrano, O., Duarte, C.M., 2021. Blue carbon as a natural climate solution. Nat. Rev. Earth Environ. 2, 826–839. https://doi.org/10.1038/s43017-021-00224-1.

Martín, A., Miloslavich, P., Díaz, Y., Ortega, I., Klein, E., Troncoso, J., Aldea, C., Carbonini, A.K., 2016. Intertidal benthic communities associated with the macroalgae *Iridaea cordata* and *Adenocystis utricularis* in King George Island, Antarctica. Polar Biol. 39, 207–220. https://doi.org/10.1007/s00300-015-1773-1.

Møller, E.F., Thor, P., Nielsen, T.G., 2003. Production of DOC by Calanus finmarchicus, C. glacialis and C. hyperboreus through sloppy feeding and leakage from fecal pellets. Mar. Ecol. Prog. Ser. 262, 185–191. https://doi.org/10.3354/meps262185.

Mystikou, A., Peters, A.F., Asensi, A.O., Fletcher, K.I., Brickle, P., van West, P., Convey, P., Küpper, F.C., 2014. Seaweed biodiversity in the south-western Antarctic Peninsula: surveying macroalgal community composition in the Adelaide Island/

Marguerite Bay region over a 35-year time span. Polar Biol. 37, 1607–1619. https://doi.org/10.1007/s00300-014-1547-1.

Norderhaug, K.M., Nygaard, K., Fredriksen, S., 2006. Importance of phlorotannin content and C : n ratio of *Laminaria hyperborea* in determining its palatability as food for consumers. Mar. Biol. Res. 2, 367–371. https://doi.org/10.1080/17451000600962789.

Norkko, A., Thrush, S.F., Cummings, V.J., Funnell, G.A., Schwarz, A.-M., Andrew, N.L., Hawes, I., 2004. Ecological role of *Phyllophora Antarctica* drift accumulations in coastal soft-sediment communities of McMurdo Sound, Antarctica. Polar Biol. 27, 482–494. https://doi.org/10.1007/s00300-004-0610-8.

Parnell, A.C., Phillips, D.L., Bearhop, S., Semmens, B.X., Ward, E.J., Moore, J.W., Jackson, A.L., Grey, J., Kelly, D.J., Inger, R., 2013. Bayesian stable isotope mixing models. Environmetrics 24, 387–399. https://doi.org/10.1002/env.2221.

Pessarrodona, A., Filbee-Dexter, K., Krumhansl, K.A., Pedersen, M.F., Moore, P.J., Wernberg, T., 2022. A global dataset of seaweed net primary productivity. Sci. Data 9, 484. https://doi.org/10.1038/s41597-022-01554-5.

Phillips, D.L., Inger, R., Bearhop, S., Jackson, A.L., Moore, J.W., Parnell, A.C., Semmens, B.X., Ward, E.J., 2014. Best practices for use of stable isotope mixing models in food-web studies. Can. J. Zool. 92, 823–835. https://doi.org/10.1139/cjz-2014-0127.

Quartino, M.L., Deregibus, D., Campana, G.L., Latorre, G.E.J., Momo, F.R., 2013. Evidence of macroalgal colonization on newly ice-free areas following glacial retreat in potter cove (South shetland Islands), Antarctica. PLoS One 8, 58223. https://doi.org/10.1371/journal.pone.0058223.

Queirós, A.M., Stephens, N., Widdicombe, S., Tait, K., McCoy, S.J., Ingels, J., Rühl, S., Airs, R., Beesley, A., Carnovale, G., Cazenave, P., Dashfield, S., Hua, E., Jones, M., Lindeque, P., McNeill, C.L., Nunes, J., Parry, H., Pascoe, C., Widdicombe, C., Smyth, T., Atkinson, A., Krause-Jensen, D., Somerfield, P.J., 2019. Connected macroalgal-sediment systems: blue carbon and food webs in the deep coastal ocean. Ecol. Monogr. 89, 01366. https://doi.org/10.1002/ecm.1366.

Reichardt, W., 1987. Burial of antarctic macroalgal debris in bioturbated deep-sea sediments. Deep-Sea Res. 34. https://doi.org/10.1016/0198-0149(87)90024-0.

Reichardt, W., Dieckmann, G., 1985. Kinetics and trophic role of bacterial degradation of macro-algae in antarctic coastal waters. Antarctic Nutrient Cycles and Food Webs. Springer Berlin Heidelberg, Berlin, Heidelberg, pp. 115–122. https://doi.org/10.1007/978-3-642-82275-9_17.

Robinson, B.J.O., Morley, S.A., Rizouli, A., Sarantopoulou, J., Gkafas, G.A., Exadactylos, A., Küpper, F.C., 2022. New confirmed depth limit of Antarctic macroalgae: palmaria decipiens found at 100 m depth in the Southern Ocean. Polar Biol. 45, 1459–1463. https://doi.org/10.1007/s00300-022-03071-y.

Saba, G.K., Steinberg, D.K., Bronk, D.A., 2011. The relative importance of sloppy feeding, excretion, and fecal pellet leaching in the release of dissolved carbon and nitrogen by *Acartia tonsa* copepods. J. Exp. Mar. Biol. Ecol. 404, 47–56. https://doi.org/10.1016/j.jembe.2011.04.013.

Schaal, G., Leclerc, J.-C., Droual, G., Leroux, C., Riera, P., 2016. Biodiversity and trophic structure of invertebrate assemblages associated with understorey red algae in a *Laminaria digitata* bed. Mar. Biol. Res. 12, 513–523. https://doi.org/10.1080/17451000.2016.1164318.

Schram, J.B., Amsler, M.O., Amsler, C.D., Schoenrock, K.M., McClintock, J.B., Angus, R. A., 2016. Antarctic crustacean grazer assemblages exhibit resistance following exposure to decreased pH. Mar. Biol. 163, 106. https://doi.org/10.1007/s00227-016-2894-y.

Simpkins, T., Van Der Mheen, M., Pedersen, M.F., Pessarrodona, A., Pattiaratchi, C., Wernberg, T., Filbee-Dexter, K., 2025. Macroalgae detritus decomposition and cross-shelf carbon export from shallow and deep reefs. Limnol. Oceanogr. 70, 1046–1058. https://doi.org/10.1002/lno.70006.

Takeuchi, I., Watanabe, K., 2002. Mobile epiphytic invertebrates inhabiting the brown macroalga, *Desmarestia chordalis*, under the coastal fast ice of Lützow-Holm Bay, East Antarctica. Polar Biol. 25, 624–628. https://doi.org/10.1007/s00300-002-0373-z.

White, L.J., Norkko, A., 2025. A path towards appropriate degradation experiments for assessing carbon sequestration potential of macroalgae. J. Ecol. https://doi.org/10.1111/1365-2745.70107.

Wiencke, C., Clayton, M.N., Gómez, I., Iken, K., Lüder, U., Amsler, C.D., Karsten, U., Hanelt, D., Bischof, K., Dunton, K., 2007. Life strategy, ecophysiology and ecology of seaweeds in polar water. Rev. Environ. Sci. Biotechnol. 6. https://doi.org/10.1007/s11157-006-9106-z.

Wiencke, C., Clayton, M.N., Schulz, D., 1995. Life history, reproductive morphology and development of the antarctic Brown Alga *Desmarestia menziesii* J. Agardh. Bot. Acta 108, 201–208. https://doi.org/10.1111/j.1438-8677.1995.tb00851.x.

Wiencke, C., Amsler, C.D., 2012. Seaweeds and their communities in polar regions. In: Wiencke, C., Bischof, K. (Eds.), Seaweed Biology: Novel Insights into Ecophysiology, Ecology and Utilization. Springer Berlin Heidelberg, Berlin, Heidelberg, pp. 265–291. https://doi.org/10.1007/978-3-642-28451-9_13.

Wiencke, C., Clayton, M.N., 2002. Synopses of the Antarctic Benthos. Koeltz Botanical Books. Germany.

Wright, L.S., Pessarrodona, A., Foggo, A., 2022. Climate-driven shifts in kelp forest composition reduce carbon sequestration potential. Glob. Change Biol. 28, 5514–5531. https://doi.org/10.1111/gcb.16299.